Journal of the European Ceramic Society **13** (1994) 143–148

Glass-Ceramics from Fly Ash with Added Li_2O

R. Cioffi, P. Pernice, A. Aronne, M. Catauro

Department of Materials and Production Engineering, Piazzale Tecchio, 80125 Naples, Italy

&

G. Quattroni

ENEL, Italian National Electricity Board, Brindisi Research Centre, Via Dalmazia 21/C, 72100 Brindisi, Italy

(Received 16 July 1993; accepted 20 September 1993)

Abstract

The effects of the addition of Li_2O to fly ash on the devitrification behaviour of the derived glass are investigated with the aid of differential thermal analysis (DTA), X-ray diffraction (XRD) and scanning electron microscopy (SEM). The phases crystallizing first for the as-quenched glass and the glass sample previously nucleated are different. Solid solutions of lithium–magnesium silicate ($Li_{(2-2x)}Mg_{(1-x)}SiO_4$) and a small quantity of β-eucryptite ($LiAlSiO_4$) solid solution are formed from the as-quenched glass, while only solid solutions of lithium–magnesium silicate are formed from the sample previously nucleated. In both cases, these crystalline phases are then converted, at higher temperatures, into a large amount of β-eucryptite solid solution together with small quantities of diopside crystals ($CaMgSi_2O_6$). Kinetic parameters for nucleation and crystal growth were estimated from the DTA curves. The temperature of maximum nucleation rate was 620 °C and the activation energy for crystal growth E = 316 kJ mol^{-1}. The crystal morphology was investigated by SEM, and the crystal shape was consistent with the morphological index n calculated by DTA. The glass ceramic obtained from a previously nucleated glass showed a fine grained texture.

Der Effekt der Zugabe von Li_2O zu Flugasche auf das Entglasungsverhalten des hergestellten Glases wurde mit Hilfe der Differentialthermoanalyse (DTA), Rontgenbeugung (XRD) und Rasterelektronenmikroskopie (SEM) untersucht. Bei Glas, das nur abgeschreckt wurde und Glas, das bereits Keime enthielt, unterscheidet sich die erste Kristallisationsphase. Es bilden sich Lithium-Magnesiumsilikat Mischkristalle ($Li_{(2-2x)}Mg_{(1-x)}SiO_4$) und geringe Mengen β-Eucrypit Mischkristall ($LiAlSiO_4$), während sich nur Lithium-Magnesiumsilikat-Mischkristalle in Proben bilden, die bereits Keime enthalten. In beiden Fallen wandeln sich diese kristallinen Phasen bei höheren Temperaturen in große Mengen β Eucryptit und geringe Mengen Diopsidkristall ($CaMgSi_2O_6$) um. Kinetische Parameter für die Keimbildung und das Kristallwachstum werden an hand der DTA-Kurven abgeschatzt. Die Keimbildungsrate erreicht ein Maximum bei 620 °C und die Aktivierungsenergie für das Kristallwachstum betrug E = 316 kJ mol^{-1}. Die Kristallmorphologie wurde mit Hilfe von SEM untersucht, die Kristallform stimmte mit dem morphologischen Index n, berechnet mit DTA, überein. Die Glaskeramik, die sich aus Glas bildet, das bereits Keime enthielt, zeigte eine feinkorn ige Textur.

On a étudié l'effet de l'addition de Li_2O aux cendres volantes sur la dévitrification du verre dérivé, ceci à l'aide d'analyse thermique différentielle (DTA), diffraction X (XRD), et microscopie à balayage (SEM). Les premières phases à cristalliser dans le verre simplement trempé et dans l'échantillon de verre nucléé au préalable sont différentes. Dans le verre simplement trempé, il se forme des solutions solides de silicate de lithium–magnesium ($Li_{(2-2x)}Mg_{1-x}SiO_4$) et une solution solide d'eucryptite β ($LiAlSiO_4$) en petite quantité, alors que dans le verre préalablement nucléé, seules les solutions solides de silicate de lithium magnésium apparaissent. Dans les deux cas, ces phases cristallines sont converties à plus haute température en un mélange d'une grande quantité de solution solide d'eucryptite β, et d'une petite quantité

Journal of the European Ceramic Society 0955-2219/94/$7.00

de cristaux de diopside ($CaMgSi_2O_6$). On a estimé les paramètres cinétiques pour la nucléation et la croissance cristalline à partir des courbes d'analyse thermique différentielle. La température maximale de nucléation est de 620° C et l'énergie d'activation pour la croissance cristalline $E = 316\ kJ\ mol^{-1}$ *La morphologie des cristaux a été observée au SEM et leur forme est en accord avec l'indice morphologique n calculé par DTA. La vitrocéramique obtenue à partir d'un verre nucléé au préalable présente une structure de grains fine*

1 Introduction

The processing of ores and fuels leaves large quantities of waste (ashes, slag, etc.), only part of which can be utilized by the cement industry As regards fly ash, the amount utilized in Italy is about 1% of cement production [1] As a consequence, new uses of fly ash have to be searched for in order to meet requirements arising from the large production and the greater attention of the community towards an adequate disposal in terms of environmental safeguard [2] Hence there is considerable interest in their utilization as starting materials for glass-ceramic production [3,4]

Moreover, coal fly ashes are much more convenient than steel slag: they are available in a fine powder form; they are ready for mixing with other ingredients in batch, and in greater quantities than slag

This work is part of a more general study having the ultimate technological objective of maximizing the amount of ashes in the batch, otherwise the production would be economically unjustified.

In previous papers[5,6] the devitrification of fly ash derived glass without the addition of any other ingredient and the effects of the addition of MgO and TiO_2 to the fly ash on the crystallization mechanism of the derived glass were studied The results of these studies have shown that the fly ash derived glass exhibits internal nucleation without the addition of any nucleating agent. A fine-grained glass-ceramic was obtained but the high viscosity of the melted glass does not allow the production of objects by the conventional techniques. On the other hand, the addition of MgO and TiO_2 to the fly ash lowers the melt viscosity but does not allow internal nucleation, as a phase separation occurs in the glassy matrix.

In this paper the effects of the addition of Li_2O to fly ash on the devitrification mechanism of the derived glass are investigated with the aid of differential thermal analysis (DTA), X-ray diffraction (XRD) and scanning electron microscopy (SEM)

2 Experimental Procedure

The glass was prepared by mixing fly ash with analytical grade reagent Li_2CO_3 in a Pt crucible so that the weight ratio of 10:0·75 of fly ash to Li_2O was obtained in the batch The composition of the fly ash, obtained from the Coal Burning Power Plant (ENEL, Porto Marghera, Venice) is reported in Table 1 The glass composition lies in the range of compositions of glass ceramic materials based on the SiO_2-Al_2O_3-Li_2O system, where the main crystalline phase is a solid solution of β-eucryptite.[7] The glass was melted in an electric oven at 1500° C for 4 h and then quenched in a cast iron mould. The as-quenched glass, annealed for 30 min at about 100° C below the glass transition temperature, was cut by a diamond saw blade in pieces suitable for the experimental measurements.

Differential thermal analysis (DTA) curves were recorded in air at different heating rates (2, 5, 7·5, 10, 20° C min^{-1}) on bulk specimens of about 50 mg. Powdered Al_2O_3 was added to improve heat transfer between the bulk sample and the sample holder. A Netzsch thermoanalyser High Temperature DSC 404 was used with Al_2O_3 as reference material The nucleation heat treatments were performed in the DTA apparatus to eliminate temperature gradients. Nucleation times were measured on isothermal DTA curves from the time at which the samples, heated at 50° C min^{-1}, reached the selected temperature

To investigate the amorphous nature of the as-quenched glass and the crystalline phases developed during the DTA runs, the thermally processed samples were finely ground The samples were analysed in a computer-assisted X-ray (CuK_α) powder diffractometer (XRD) using a Philips diffractometer model PW1710, with a scan speed of 1° min^{-1}. Using a built-in computer search program, the X-ray diffraction patterns were matched to JCPDS data and corresponding phases were identified.

For the investigation of the glass-ceramic texture and crystal morphology, a scanning electron microscope, Cambridge model S-240, was used Samples were mounted in epoxy and surfaces were ground

Table 1. Coal fly ash composition

Oxide	*wt %*
SiO_2	48·72
Al_2O_3	35·79
Fe_2O_3	3·72
CaO	8·10
MgO	1·40
K_2O	0·57
Na_2O	0·16
TiO_2	1·54

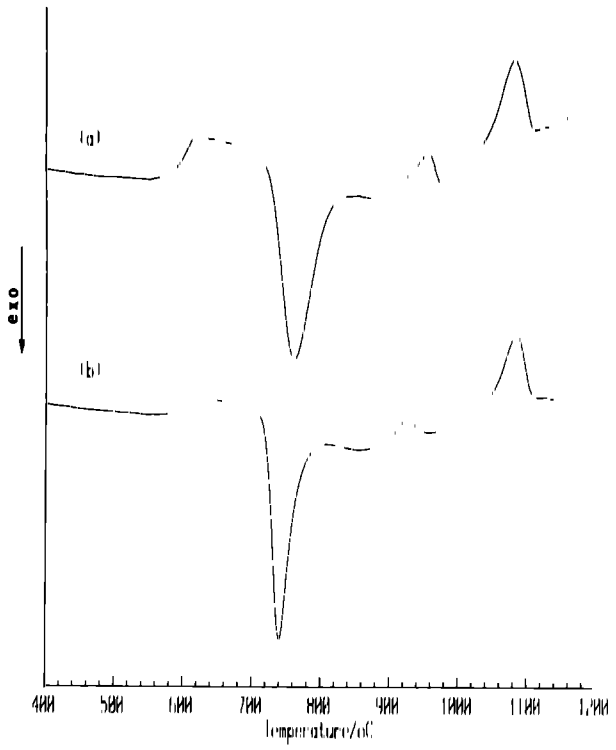

Fig. 1. DTA curves of the investigated glass recorded at 10 °C min^{-1} (a) as quenched sample (b) sample nucleated for 12 h at 620 °C

smooth, then polished with diamond paste. Samples were etched in 1% HF for approximately 60 s. The etched samples were coated with a thin Au film.

3 Results and Discussion

3.1 DTA and X-ray diffraction

The DTA curves carried out on (a) a bulk sample of the as quenched glass and (b) a sample previously nucleated are reported in Fig. 1. A slope change occurs at the same temperature on both curves followed by one exothermic effect, with a maximum at 761 °C in Fig. 1(a) and at 740 °C in Fig. 1(b), followed at higher temperatures by two endothermic effects. The second endo-peak occurs at about the same temperature, 1080 °C, on both curves, while the maximum of the first endo-peak shifts from 957 °C in Fig. 1(a) to 924 °C in Fig. 1(b). The slope change may be attributed to the glass transition. In this work, the inflection point of the DTA curve was taken as the glass transition temperature (T_g = 593 °C).

To investigate the nature of the thermal effects on the DTA curves, XRD analysis was performed. The XRD patterns of the as quenched glass have broad humps characteristic of the amorphous state. The XRD patterns of a sample heated up to the temperature of the exo peak (a) and of the samples heated in the DTA furnace until the maximum (b) and until to the end (c) of the first endo peak, are reported in Fig. 2. Many reflections appear in Fig. 2(a), indicating that the exo peak on the DTA curve of the as quenched glass is related to a crystallization process. These reflections were assigned to a solid solution of β-eucryptite ($LiAlSiO_4$) and solid solutions of lithium-magnesium silicate ($Li_{(2-2x)}Mg_{(1+x)}SiO_4$), even if, for a few reflections, the agreement between the intensity values experimentally obtained with ones reported on the JCPDS cards is not complete.

The progressive decrease of the reflections attributed to solid solutions of lithium-magnesium silicate and the simultaneous increase of ones corresponding to a solid solution of β-eucryptite, together with the appearance of the main reflections of diopside crystals ($CaMgSi_2O_6$), going from Fig. 2(a) to (c) shows that the first endo-peak of the DTA curve of the as quenched glass is due to the transformation process of solid solutions of lithium-magnesium

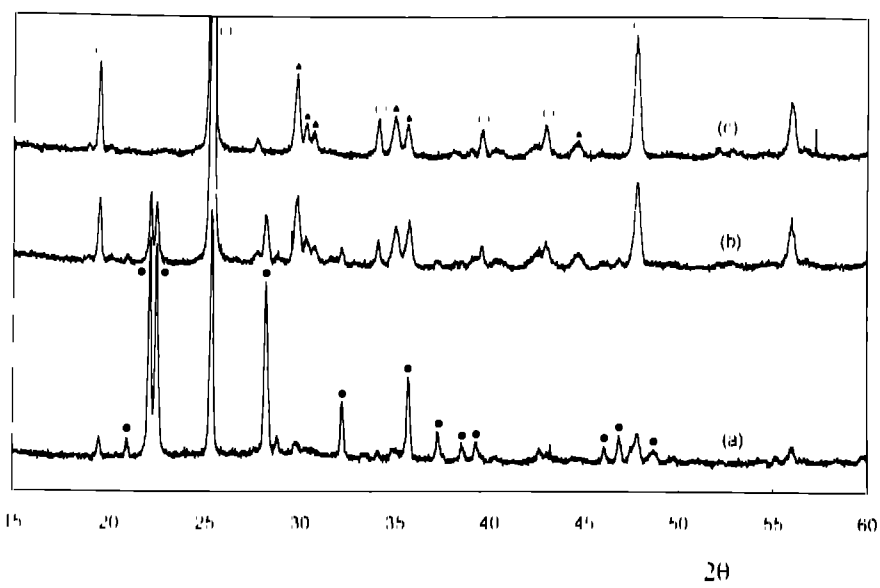

Fig. 2. X Ray diffraction patterns of samples heated (a) to the temperature of the DTA exo peak, (b) to the maximum of the first DTA endo peak and (c) to the end of the first DTA endo peak (●) Lithium-magnesium silicate solid solutions (▲) diopside crystals, (○) β eucryptite solid solution

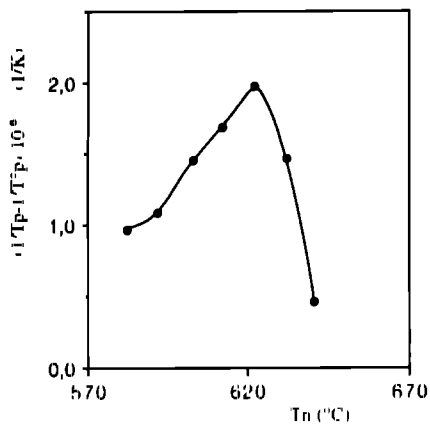

Fig. 3. Nucleation rate-temperature like curve

silicate, by reaction with the residue glassy matrix, into a large amount of solid solution of β-eucryptite and, in less quantity, into diopside crystals. The second endo-peak of the DTA curves of the as-quenched glass and of the previously nucleated sample occurs in the same temperature range Moreover, the look of the XRD pattern of a sample after a DTA run is very similar to that shown by the sample heated until the end of the first endo-peak, see Fig. 2(c), indicating that the second endo peak on both DTA curves may be attributed to melting of the crystals previously obtained

3.2 Temperature of maximum nucleation rate

As reported by Marotta *et al*,[8] a nucleation rate-temperature-like curve can be obtained from DTA curves, recorded at the same heating rate, of the samples with the same specific surface This method is based on the shift of the DTA crystallization peak temperature, T_p, from that of the as-quenched glass, T_p', as a consequence of the heat treatment of nucleation at different temperatures If the samples are held the same time (t_n = 2 h) at each temperature (T_n) of the heat treatment, a plot of $(1/T_p - 1/T_p')$ against the temperature T_n of the nucleation heat treatment (Fig. 3) gives a nucleation rate-temperature-like curve that exhibits a maximum at the temperature of 620°C.

The XRD patterns of the sample nucleated (12 h) at the temperature of the maximum nucleation rate (a), the same sample heated to the temperature of the exo peak (b), and then heated to the temperature of the first endo-peak of the DTA curve (c), are reported in Fig. 4. Figure 4(a) shows that the heat-treatment of nucleation does not cause crystallization. Figure 4(b), if compared with Fig 2(a), does not exhibit the reflections assigned to the solid solution of β-eucryptite but only shows the reflections assigned to solid solutions of lithium-magnesium silicate. At higher temperatures, see Fig 4(c), the transformation of the solid solutions of lithium-magnesium silicate into the solid solution of β eucryptite and a small quantity of diopside crystals takes place This result may be interpreted on the basis of the different structures of the crystalline phases obtained. They contain the same structural unit, the orthosilicate anion (SiO_4^{4-}), arranged in different ways. Isolated tetrahedra form the structure of the lithium-magnesium silicate phases, while chains and framework of tetrahedra make up the structures of diopside and β eucryptite phases, respectively The nucleation heat-treatment causes the crystallization of more depolymerized phases, according to the composition of the mother glass, that are more kinetically favoured than more complicated structures of diopside and β eucryptite phases Moreover, the nucleation heat-treatment gives rise to a remarkable difference in the glass-ceramic texture. As shown in Fig. 5, which shows

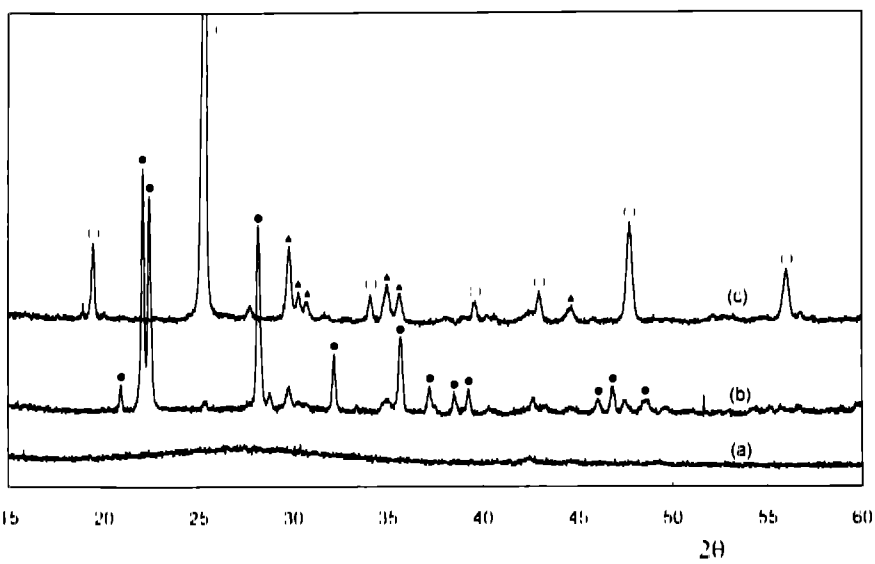

Fig. 4. X Ray diffraction patterns of the sample (a) nucleated for a long time (12 h) at the temperature of the maximum nucleation rate, (b) heated to the temperature of the DTA exo peak, (c) heated to the temperature of the first DTA endo peak. (●) Lithium-magnesium silicate solid solutions, (▲) diopside crystals, (○) β eucryptite solid solution.

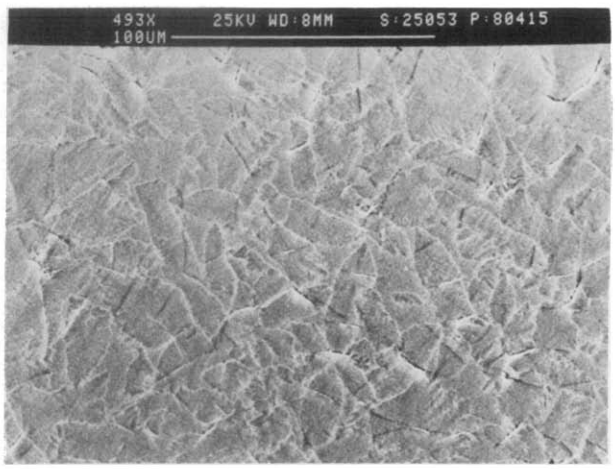

(a)

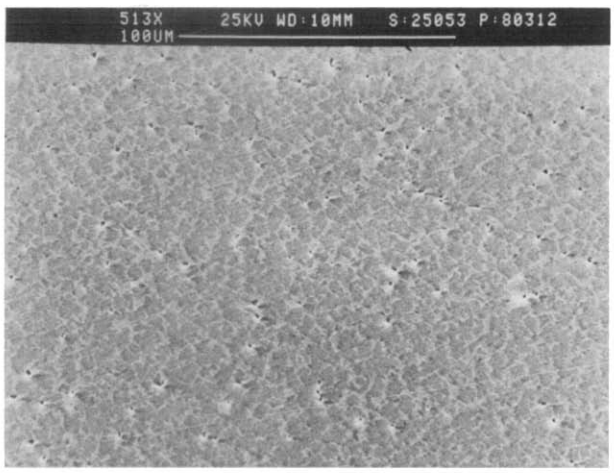

(b)

Fig. 5 SEM photomicrographs of samples heated to the temperature of the DTA exo peak (a) as quenched glass (b) sample nucleated for 12 h at 620 °C

SEM photomicrographs of a non nucleated sample (a), and a nucleated sample (b), the previously nucleated sample exhibits a finer-grained texture than the non nucleated sample.

Finally, the transformation process into the solid solution of β eucryptite for the as-quenched glass or for the glass sample previously nucleated, yields a glass-ceramic material with high crystallinity but strongly fractured as consequence of the large variation of volume that takes place in this transformation, as shown in Fig. 6

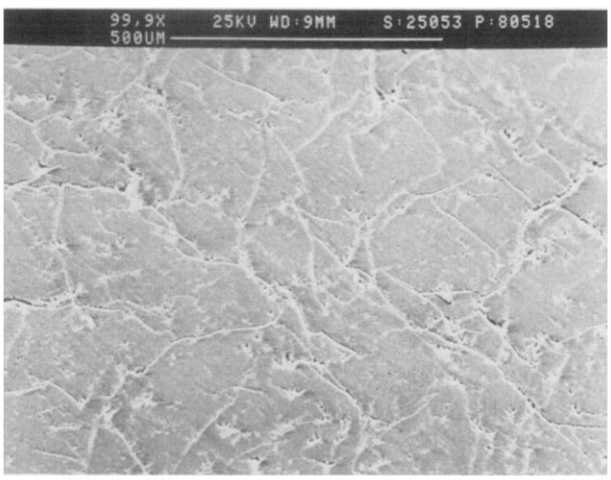

Fig. 6. SEM photomicrograph of a sample heated to the temperature of the first DTA endo peak

3.3 Kinetic parameters of crystal growth

When DTA runs are carried out on bulk (low specific surface area) samples previously nucleated for a long time at the temperature of a high nucleation rate the crystals grow at each heating rate from the same number of nuclei, i.e. the number of nuclei formed during the DTA run can be regarded as negligible.[8]

As samples of the studied glass were nucleated for 12 h at the temperature of the maximum nucleation rate as detected on the nucleation rate-temperature like curve, the following equation can be used [9]

$$\ln \beta = \left(\frac{E}{R}\right)\left(\frac{1}{T_p}\right) + \text{constant} \qquad (1)$$

where β is the DTA heating rate, E is the activation energy for crystal growth and T_p is the temperature of a maximum of the DTA crystallization peak. A value of activation energy, $E = 316\ \text{kJ mol}^{-1}$, for the crystal growth, was calculated from the slope of the straight line obtained by plotting $\ln \beta$ against $1/T_p$, see Fig. 7. The value of the morphological index, n, that is related to the crystal shape (rod-like $n = 1$; plate-like $n = 2$, three dimensional $n = 3$) can be evaluated, using the value of E previously calculated, from the following equation [10]

$$nE = -\frac{1.92}{\left(\frac{1}{T_{i1}} - \frac{1}{T_{i2}}\right)} \qquad (2)$$

where T_{i1} and T_{i2} are the two inflection point temperatures, corresponding to the crystallization peak detected from the derivative of the DTA curve of a sample previously nucleated. A value found, 2.8,

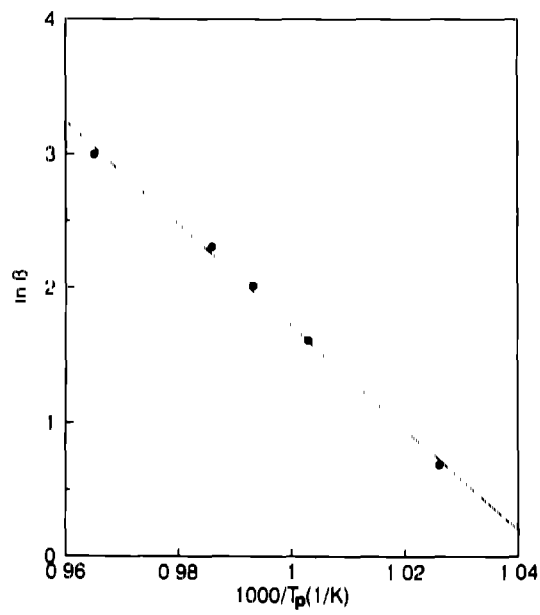

Fig. 7. Plot of $\ln \beta$ versus $1/T_p$

is consistent with the morphology of the crystalline phases obtained from the heat-treatment of nucleation, i.e. three-dimensional crystals of lithium-magnesium silicate solid solutions.

4 Conclusions

From the experimental results the following conclusions can be drawn. The investigated glass exhibits internal nucleation with a maximum nucleation rate at 620°C. The devitrification process occurs in two steps. Initially, samples nucleated for a long time, unlike as-quenched samples, in which a small amount of β-eucryptite solid solution also crystallizes, only lithium-magnesium silicate solid solutions crystallize. The activation energy of this step is $E = 316\ \mathrm{kJ\ mol^{-1}}$. At higher temperatures the lithium-magnesium silicate solid solutions are converted, in a large amount, into β-eucryptite solid solution, and in a small quantity, into diopside crystals. This transformation produces a fine-grained glass-ceramic material with a high crystallinity degree but strongly fractured.

References

1 Puccio, M., *Le ceneri di carbone* ITEC, Milan, 1983, p. 49.
2 Hemmings, R. T. & Berry, E. E., On the glass in coal fly ash: recent advances. In *Mat. Res. Soc. Symp. Proc.*, Vol. 113, ed. G. J. McCarthy, F. P. Glasser, D. M. Roy & R. T. Hemmings. Materials Research Society, Pittsburgh, PA, 1988, pp. 3–38.
3 DeGuire, E. J. & Risbud, S. H., Crystallization and properties of glasses prepared from Illinois coal fly ash. *J. Mater. Sci.*, **19** (1984) 1760–6.
4 Cumpston, B., Shadman, F. & Risbud, S., Utilization of coal ash minerals for technological ceramics. *J. Mater. Sci.*, **27** (1992) 1781–4.
5 Cioffi, R., Pernice, P., Aronne, A., Marotta, A. & Quattroni, G., Nucleation and crystal growth in a fly ash derived glass. *J. Mater. Sci.*, to be published.
6 Cioffi, R., Pernice, P., Aronne, A., Marotta, A. & Quattroni, G., Phase separation and crystallization in a fly ash derived glass. *J. Non-Cryst. Solids*, to be published.
7 Strnad, Z., *Glass Ceramic Materials* Elsevier, Amsterdam, 1986, pp. 85–97.
8 Marotta, A., Buri, A. & Branda, F., Nucleation in glass and differential thermal analysis. *J. Mater. Sci.*, **16** (1981) 341–4.
9 Ozawa, T., Kinetics of non-isothermal crystallization. *Polymer*, **12** (1971) 150–8.
10 Marotta, A., Saiello, S., Branda, F. & Buri, A., Activation energy for the crystallization of glass from DDTA curves. *J. Mater. Sci.*, **17** (1982) 105–8.